Available online at www.sciencedirect.com

ScienceDirect

journal homepage: www.elsevier.com/locate/issn/15375110

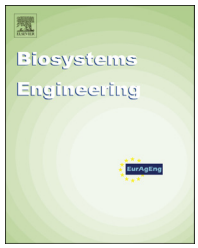

Research Paper

Validation of top electrode voltage in free-running oscillator radio frequency systems with different moisture content soybeans

Kun Wang [a], Hankun Zhu [a], Long Chen [a], Wei Li [a], Shaojin Wang [a,b,*]

[a] College of Mechanical and Electronic Engineering, Northwest A&F University, Yangling, Shaanxi 712100, China
[b] Department of Biological Systems Engineering, Washington State University, Pullman, WA 99164-6120, USA

ARTICLE INFO

Article history:
Received 24 June 2014
Received in revised form
14 October 2014
Accepted 12 January 2015
Published online

Keywords:
RF
Top electrode voltage
Moisture content
Finite element simulation
Soybean

Precisely estimating the top electrode voltage of a radio frequency (RF) system is important for computer simulation of sample temperatures. The goal of this study was to validate whether the developed equations can be applied to determine the top electrode for RF heated soybeans with different moisture contents. Soybeans with moisture contents of 6.7% and 8.7% (w.b.) were treated in a 27.12 MHz, 6 kW RF system under 5 electrode gaps. The results showed that the top electrode voltage increased almost linearly both with increasing moisture content and decreasing electrode gap. The maximum difference of the estimated top electrode voltages was less than 10% relative error between the anode current and the measured current in the same conditions. The temperature distributions in three representative layers from simulation were in good agreement with those from experiment, as was the average root mean square error (RMSE) of 1.6% for temperature profiles in three selected positions. The validation results demonstrated that the established equation using anode current was suitable for estimating the top electrode voltage when soybeans of different moisture contents were heated in RF systems.

1. Introduction

Dielectric heating using radio frequency (RF) energy has been increasingly studied in recent years because of the rapid and volumetric heating, large power penetration depth, and high energy efficiency (Jiao, Tang, Wang, & Koral, 2014; Liu, Yang, & Mao, 2010; Piyasena, Dussault, Koutchma, Ramaswamy, & Awuah, 2003). Two types of RF systems, including 50 Ω and free-running oscillator, are widely used for laboratory researches and industrial applications. Since 50 Ω units are expensive, the free-running oscillator RF system has been widely applied for thawing (Farag, Lyng, Morgan, & Cronin, 2008, 2011), post-baking (Koral, 2004; Koray, Coşkun, Kocadağlı, & Gökmen, 2012), disinfestation (Lagunas-Solar et al., 2007; Shrestha & Baik, 2013; Wang, Monzon, Johnson, Mitcham, & Tang, 2007a, 2007b; Wang, Tiwari, Jiao, Johnson, & Tang, 2010), drying (Lee, Li, Zhao, & Park, 2010; Marshall & Metaxas, 1999; Wang, Zhang, et al. 2013) and pasteurisation (Gao, Tang, Villa-Rojas, Wang, & Wang, 2011; Kim, Sagong,

* *Corresponding author*. College of Mechanical and Electronic Engineering, Northwest A&F University, Yangling, Shaanxi 712100, China. Tel.: +86 29 87092319; fax: +86 29 87091737.
E-mail address: shaojinwang@nwsuaf.edu.cn (S. Wang).
http://dx.doi.org/10.1016/j.biosystemseng.2015.01.001
1537-5110/

Choi, Ryu, & Kang, 2012). However, the major challenges for commercial RF applications are non-uniform and run-away heating, such as overheating in corners and edges (Fu, 2004; Tiwari, Wang, Tang, & Birla, 2011; Uyar, Erdogdu, & Marra, 2014; Wang et al., 2010; Wang, Tang, Johnson, & Cavalieri, 2013). To improve final temperature distributions, computer simulation has been effectively used to help understand the complex RF heating mechanism and optimise the RF heating process (Huang, Zhu, Yan, & Wang, 2015). One of the important parameters is to determine the top electrode voltage for a specific product in the RF heating simulation.

The voltage is assumed to be uniformly distributed over the top electrode because the dimensions of the top electrode are designed to be less than 30% of the RF wavelength (11 m) at 27.12 MHz (Barber, 1983). Metaxas (1996) reported that the voltage varies by only 7% between standby and full load for a typical industrial-scale RF system. The voltage value is a function of the top electrode configuration, electrode gap and load conditions, and could be determined by analytical methods (Birla, Wang, & Tang, 2008; Jiao et al., 2014), computer simulations (Alfaifi et al., 2014; Marshall & Metaxas, 1998; Tiwari et al., 2011) and direct measurements (Zhu, Huang, & Wang, 2014). The analytical method could be simply used to calculate the top electrode voltage when the measured heating rate is determined. But its accuracy is dependent on the average heating rate over the heating volume, which is difficult to be representative for the limited temperature measurement locations from the non-uniform heating fields (Birla et al., 2008). The computer simulation is also applied to estimate the top electrode voltage by the trial and error approach based on the matching degree of RF heating patterns in three layers (Alfaifi et al., 2014). The estimation accuracy is usually poor since the matching degree is evaluated qualitatively both in patterns and absolute temperature differences (Tiwari et al., 2011). Recently, Zhu et al. (2014) developed two correlations based on the directly measured current and the anode current to quickly estimate the top electrode voltage used for computer simulation, which have been validated both by analytical and simulation methods for the soybeans at 4.7% moisture content. Further validation studies are needed for general applications of the regressed equations.

The RF heating behaviour depends on the thermal and dielectric properties of soybeans while the electrode configuration is fixed (Jiao et al., 2014). These physical properties are mainly influenced by the moisture content in samples (Alam & Shove, 1973; Deshapande & Bal, 1999; Deshapande, Bal, & Ojha, 1996; Guo, Wang, Tiwari, Johnson, & Tang, 2010), resulting in various top electrode voltages. To obtain effective final temperature distributions, it is important to evaluate the top electrode voltage estimated by the anode and the measured currents to be suitable for RF treated soybeans with different moisture contents.

The objectives of this research were to: (1) obtain the anode current (I_a) and the measured current (I_m) when soybeans with different moisture contents were treated in RF systems under various electrode gaps, (2) apply the estimated top electrode voltage to simulate the RF heating using commercial finite element software COMSOL, and (3) compare the experimental and simulated temperature distributions to validate the estimated top electrode voltage.

2. Materials and methods

2.1. RF heating systems

A free-running oscillator, 6 kW, 27.12 MHz pilot-scale RF heating system (SO6B, Strayfield International, Wokingham, U.K.) was used for the RF heating experiment. This applicator system had two parallel plate electrodes. The size of top electrode was 400 mm (W) × 830 mm (L), and the feed strip was located at the middle of the backside on the top electrode plate. The gap between the two parallel plates was adjusted to change RF output power and thus, the top electrode voltage. The anode current displayed on the screen of the RF system was used to calculate the top electrode voltage.

2.2. Materials and sample preparation

Soybeans (*Glycine max*) were purchased from a local supermarket in Yangling, Shaanxi, China. The initial moisture content of soybeans was 4.7% on wet basis (w.b.). Based on the moisture content of samples used in previous study (Zhu et al., 2014), two other moisture contents of 6.7% (w.b.) and 8.7% (w.b.) were selected in this validation experiment. The initial samples were conditioned by direct addition of a predetermined amount of distilled water to obtain the target moisture contents. The preconditioned samples were gently mixed and shaken by hand for 15 min. The samples were sealed in air-tight plastic bags and stored at 4 °C for 4 days in a refrigerator to allow the moisture to equilibrate. During the storage, the bags were shaken 4 times per day. Four days later, the sample bags were taken out from the refrigerator and put in an incubator to equilibrate at 25 °C for one more day before the experiment (Guo et al., 2010; Guo, Tiwari, Tang, & Wang, 2008; Rani, Chelladurai, Jayas, White, & Kavitha-Abirami, 2013).

2.3. RF heating procedure

Samples were removed from the incubator immediately to have a uniform initial temperature (25 °C) prior to RF heating. The 3 kg soybean samples in a polypropylene container (300 mm L × 220 mm W × 85 mm H) with perforated side and bottom walls were placed in the centre of the bottom electrode. The soybeans in the container were divided into three layers and separated by two thin gauzes (with mesh opening of 1 mm) to easily map the sample temperatures at heights of 2, 4 and 6 cm (Fig. 1) after RF treatments. The RF heating was conducted at five electrode gaps of 11.0, 11.5, 12.0, 12.5, and 13.0 cm as used by Zhu et al. (2014), without conveyor belt movement.

The initial anode currents were read directly from the control screen of the RF unit and recorded immediately after the RF power was turned on. The measured currents were determined by a measuring device, which mainly consisted of voltage divider, filter and measuring parts. A detailed description of the measuring device can be found in Zhu et al. (2014). Three decimal point readings from the ammeter were required to ensure the reading accuracy of the current value.

During the RF heating, sample temperatures at three representative locations (Fig. 1) in the container were

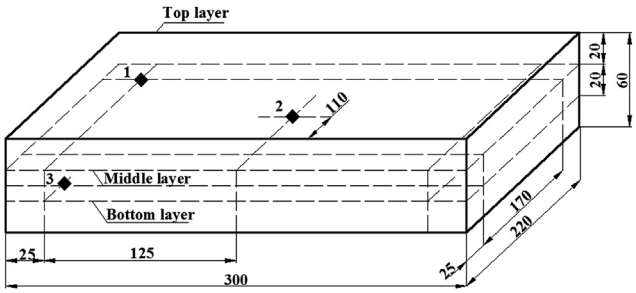

Fig. 1 – Temperature measurement locations (1–3) (points 1 and 2 were at the surface of middle layer and point 3 was at the surface of bottom layer) of fibre optic sensors and three layers for thermal imaging cameras in the sample container. All dimensions are in mm.

measured using fibre optic sensors (FTS-P104, HeQi Opto-Electronic Technology, Xi'an, Shaanxi, China) with an accuracy of ±1 °C. When the sample temperature in the location 2 (the centre of the middle layer) reached 47 °C, resulting in about 52 °C for the average sample temperature determined in the preliminary experiment, the RF unit was turned off and the container was immediately moved out for the surface temperature measurement. The surface temperatures were measured with a digital infrared camera (DM63, Dali Science and Technology, Hangzhou, Zhejiang, China) with an accuracy of ±2 °C, which was obtained after calibrations against a thermocouple thermometer (HH-25TC, Type-T, OMEGA Engineering Inc., Stamford, Connecticut, USA) with an accuracy of ±0.5 °C. Details on measurement procedure and the precision of this type of camera can be found elsewhere (Birla, Wang, Tang, & Hallman, 2004; Tiwari, Wang, Birla, & Tang, 2008; Wang, Birla, Tang, & Hansen, 2006; Wang et al., 2010; Zhu et al., 2014). Thermal images were taken of the upper surface of soybeans, beginning with the top layer working towards the bottom one. The total measurement time for the three layers was about 15 s. From each of the thermal images, 44,250 individual surface temperature data points were collected over a sample surface in the container and were used for statistical analyses (Wang et al., 2007b; Wang, Tang, et al., 2013; Wang, Zhang, et al., 2013; Wang, Yue, Tang, & Chen, 2005). Each test was repeated two times.

2.4. *Simulation using the estimated top electrode voltage*

Based on the anode currents (I_a, A) and measured currents (I_m, A) observed above, the top electrode voltages (V, V) were estimated by the following equations developed by Zhu et al. (2014):

$$V = 11242 \times I_a + 2029.9 \quad (1)$$

$$V = -22760 \times I_m + 7384.2 \quad (2)$$

The voltages estimated by the anode currents were applied to simulate the RF heating using commercial finite element software COMSOL (V4.3a, COMSOL Multiphysics, Burlington, MA, USA) and the voltages estimated by the measured currents could be used as reference values for comparison. The electric field intensity in the electromagnetic field was solved by the Laplace equations simplified from Maxwell's electromagnetic field equations since the wavelength (11 m) of electromagnetic wave in the 27.12 MHz RF system is usually much larger than the RF cavity size. The temperature distributions in RF heated soybeans with two moisture contents were simulated by combining the electromagnetic and heat transfer equations using Joule heating model under different electrode gaps.

The top uncovered surface of the sample was assumed to have convective heat transfer (h = 20 W m^{-2} K^{-1}) by free convection of ambient air (Wang, Tang, & Cavalieri, 2001). Other outer surfaces of the plastic container were considered as thermally insulated ($\nabla T = 0$). The soybean samples were equilibrated at room temperature (25 °C) in the incubator prior to RF heating, which was set as the initial temperature in the simulation. The dielectric, thermal, and physical properties of the bulk sample (soybean), container (polypropylene), and the surrounding medium (air) are important parameters for simulation and are listed in Table 1. Detailed geometrical and electrical boundary conditions of RF systems can be found elsewhere (Alfaifi et al., 2014; Tiwari et al., 2011). Fine tetrahedral mesh was created in the soybean sample and the top electrode to guarantee the accuracy of temperature distribution results. Other parts of the system used a normal size tetrahedral mesh. The mesh system was refined sequentially until the difference in the resulting temperatures between successive calculations was less than 0.1%. Initial and maximum time steps were set as 0.001 and 1 s, respectively. The software was run on a Dell workstation with two Dual Core 3.10 GHz Xeon processors, 8 GB RAM on a Windows 7 64 bit operating system. Each simulation task took about 3 min to complete.

2.5. *Validation of the estimated top electrode voltage*

The estimated top electrode voltages based on the soybeans at 6.7% and 8.7% w.b. were used to validate the RF heating in soybeans at different moisture levels. The validation was conducted both using the temperature distributions in the

Table 1 – Thermal and dielectric properties of materials used in the computer simulation.

Properties	Bulk soybean at moisture content (w.b.)		Polypropylene container[c]	Air[c]
	6.7%	8.7%		
Density (kg m^{-3})	750	740	900	1.2
Heat capacity (J kg^{-1} K^{-1})	1837[b]	1954[b]	1800	1200
Thermal conductivity (W m^{-1} K^{-1})	0.111[b]	0.118[b]	0.2	0.025
Dielectric constant	2.80[a]	3.28[a]	2.0	1.0
Dielectric loss factor	0.154[a]	0.245[a]	0.0023	0.0

[a] Guo et al. (2010).
[b] Deshapande and Bal (1999), Deshapande et al. (1996).
[c] COMSOL material library, V4.3a (2012).

three layers and the temperature-time histories at the three representative locations (Fig. 1) in simulation and experiment. For the surface temperature distribution in the three layers, the experimental and simulated temperature (°C) distributions of soybeans with 6.7% w.b. moisture content at an electrode gap of 120 mm were selected as an example to make a comparison. For temperature distributions of the three selected positions, the experimental and simulated temperature–time histories of the RF heated soybeans were compared at five electrode gaps and two moisture contents.

The temperature distributions were qualitatively analysed by isothermal contour plots. To better understand the difference between the experimental and simulated temperature profiles, the root mean square error (RMSE, %) was used to evaluate the simulation accuracy as follows (Huang et al., 2014):

$$RMSE = \sqrt{\frac{1}{N}\sum_{i=1}^{N}((T_E(i) - T_S(i))/T_E(i))^2} \quad (3)$$

where T_E is the experimental temperature (°C), T_S is the simulated temperature (°C), i is the data number, and N is the total number of data points.

3. Results and analyses

3.1. Electric current as a function of electrode gaps

The heating times of the soybeans at the moisture content of 6.7% (8.7%) were 239, 295, 345, 414 and 477 s (186, 222, 264, 312 and 360 s) with the corresponding five electrode gaps of 110, 115, 120, 125 and 130 mm, respectively, suggesting that the heating time decreased with reducing gaps or increasing moisture content. The anode current and measured current as a function of the electrode gap are shown in Fig. 2. In the range of the tested electrode gaps (110–130 mm), anode current decreased with increasing electrode gap, but the measured current increased with increasing electrode gap at given moisture content due to the reversed original circuit design. These results can be well explained by the positive correlation with the anode current in Eq. (1) but a negative correlation with the measured current in Eq. (2). Correspondingly, the anode current increased with increasing moisture content but measured current decreased with increasing moisture content. The current trend at the two moisture levels was in good agreement with that at the original moisture content (4.7% w.b., Zhu et al., 2014).

Considering the anode current trend, Jiao, Johnson, Tang, and Wang (2012), Wang, Tang, et al. (2013), Wang, Zhang, et al. (2013), and Zhu et al. (2014) reached similar results in similar RF heating systems. However, the absolute values of the anode currents in Jiao et al. (2012) and Wang, Tang, et al. (2013), Wang, Zhang, et al. (2013) were larger than those in this study, which was probably caused by relatively higher moisture content or larger loss factor of the samples they used.

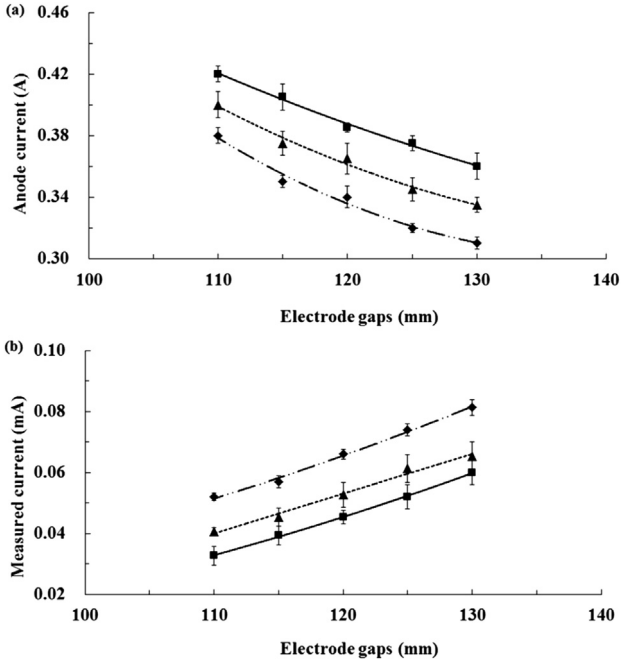

Fig. 2 – Anode current (a) and measured current (b) as a function of electrode gaps with a load of 3 kg soybeans at 4.7% (◆), 6.7% (▲) and 8.7% (■) (w.b.) moisture content.

3.2. Voltage as influenced by moisture content

Figure 3 shows the top electrode voltages estimated by the anode current or measured current as a function of moisture content for 3 kg soybeans at 5 electrode gaps. The voltage increased almost linearly with increasing moisture

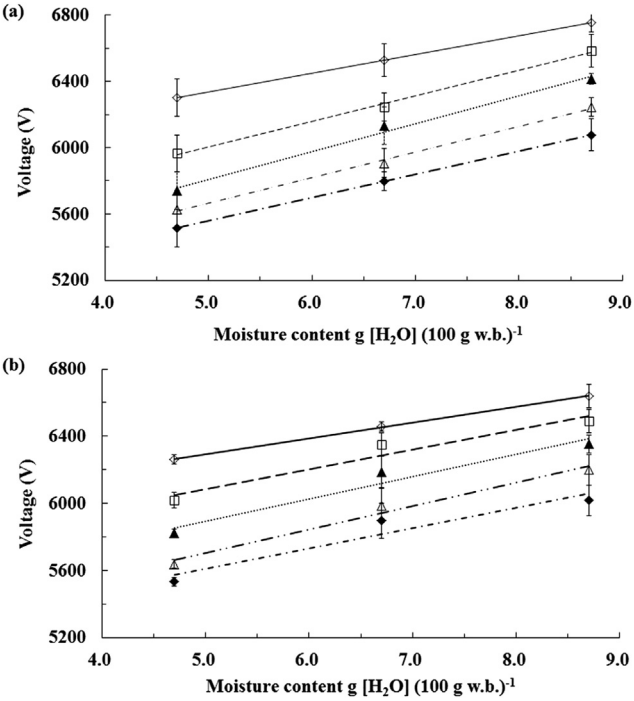

Fig. 3 – The top electrode voltages estimated by the anode current (a) or measured current (b) as a function of moisture content with a load of 3 kg soybeans under 5 electrode gaps, 110 mm (◇), 115 mm (□), 120 mm (▲), 125 mm (△) and 130 mm (◆).

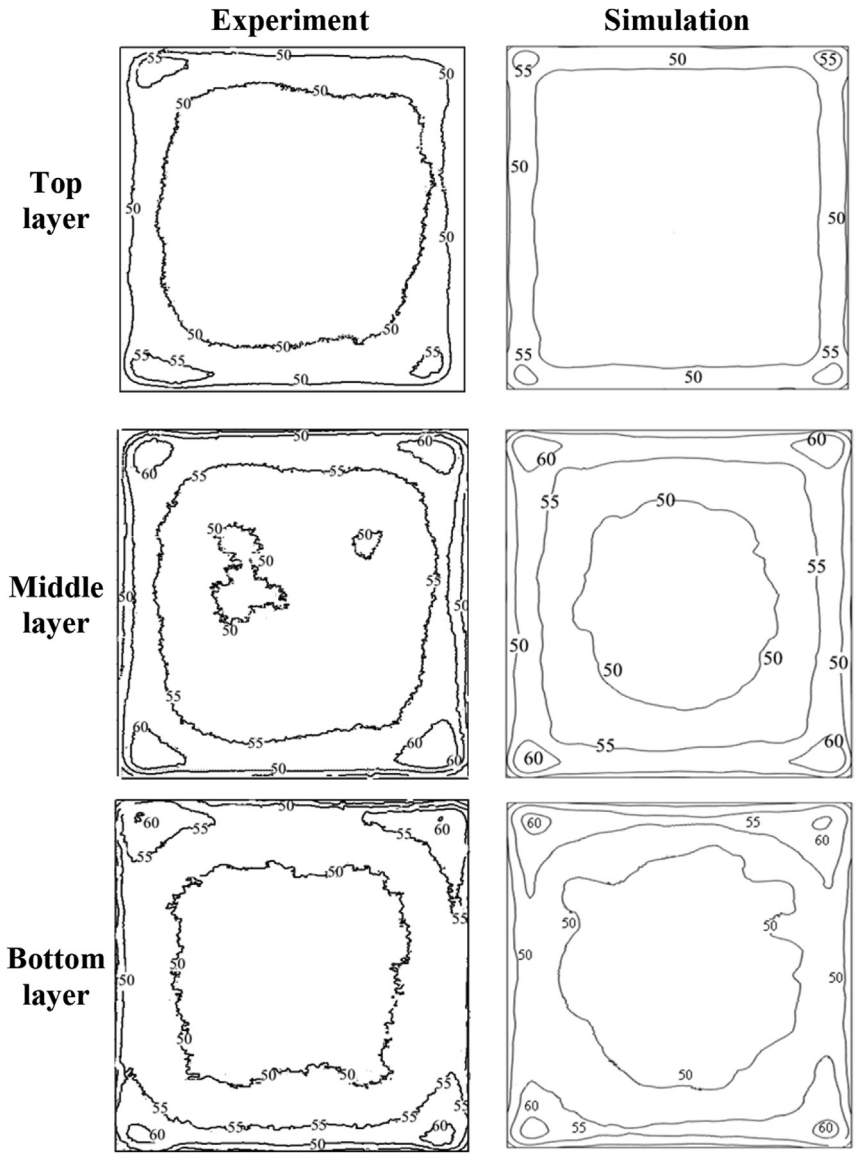

Fig. 4 – Experimental and simulated temperature (°C) distributions in top, middle, and bottom layers (20, 40, and 60 mm from the bottom of sample) of soybeans with 6.7% (w.b.) moisture content placed in a polypropylene container after 5.9 min RF heating at an electrode gap of 120 mm.

content or decreasing electrode gap. The maximum difference of the estimated top electrode voltages between the anode current and the measured current in the same conditions reached 111 V, indicating less than 10% relative error. The top electrode voltage from the measured current was in a relatively small range as compared to that from the anode current. Considering the estimated values of the top electrode voltage, Jiao et al. (2014) and Tiwari et al. (2011) reached 17,000 V and 13,000 V for heating salt solution and wheat flour, respectively, which are higher than that in this study. Alfaifi et al. (2014) and Birla et al. (2008) reported 4100 V and 8162 V for RF heating raisins and gels, respectively, which are close to the values in this study.

3.3. *Validation of the top electrode voltage by experiment and simulation*

Figure 4 shows experimental and simulated temperature distributions in top, middle, and bottom layers of soybeans with 6.7% (w.b.) moisture content placed in the polypropylene container after 5.9 min RF heating at the electrode gap of 120 mm. Both heating patterns showed that the high temperature values were located at the corners and edges of all layers while low ones were in the centre, which showed non-uniform RF heating (Alfaifi et al., 2014; Birla et al., 2008; Tiwari et al., 2011; Wang, Luechapattanaporn, & Tang, 2008). This behaviour could be attributed to the uneven distribution of the electromagnetic field and the field bending at the corners and

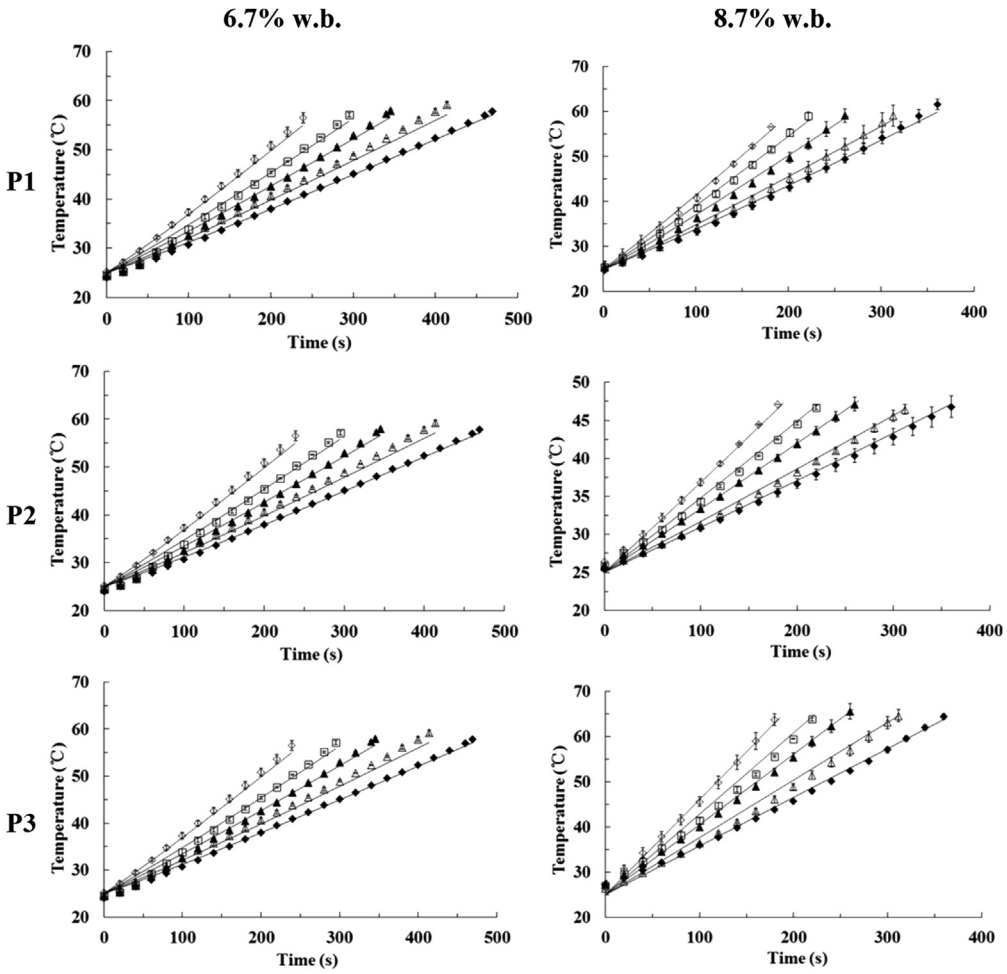

Fig. 5 – Temperature profile comparisons between experiment (symbol) and simulation (line) at three selected positions as a function of electrode gaps (110 mm "⋄", 115 mm "□", 120 mm "▲", 125 mm "△" and 130 mm "◆") at two moisture contents of soybeans.

edges of the sample (Alfaifi et al., 2014). Specifically, the average surface temperatures of the top, middle and bottom layers were 50.86 ± 1.56 °C, 53.21 ± 0.76 °C and 52.96 ± 1.16 °C by experiment, and 51.59 °C, 53.65 °C and 53.07 °C by simulation. The surface temperatures for the top layer were lower than those of the middle and bottom layers, probably because the top layer was exposed to the ambient air. Generally, the results demonstrated that simulated and experimental temperature distribution patterns matched well for all three layers, validating that the top electrode voltages estimated by the developed equations were precisely applied in the computer simulation.

The experimental and simulated temperature–time histories of the RF heated soybeans are shown in Fig. 5 at the three selected locations as influenced by electrode gaps and moisture contents. The simulated temperature profile was in good agreement with the experimental one at each electrode gap and moisture level, resulting in similar heating rates. The heating rate decreased with increasing electrode gap and decreasing moisture content, which was probably caused by the reduced RF power coupled into the sample (Zhu et al., 2014). The root mean square error (RMSE, %) between experimental and simulated temperatures of soybeans at two moisture levels and 3 selected positions calculated by Eq. (3) was listed in Table 2. The average and maximum RMSEs were 1.6% and 3.5%, respectively, suggesting that the top electrode voltages estimated by the developed Eqs. (1) and (2) were accurate for computer simulation. The validated results further proved that the electric currents in samples with different moisture levels could be precisely and quickly

Table 2 – Root mean square error (RMSE, %) between experimental and simulated temperatures of soybeans at two moisture levels and 3 selected positions.

Gap (mm)	Positions with moisture content of 6.7% w.b.			Positions with moisture content of 8.7% w.b.		
	P1	P2	P3	P1	P2	P3
110	1.26	0.80	2.57	1.14	1.39	0.85
115	3.22	1.02	3.50	1.44	1.26	3.10
120	2.60	0.43	1.59	1.62	0.98	2.30
125	1.96	0.46	0.98	1.73	1.13	2.71
130	1.53	0.54	0.86	1.56	0.92	3.46

applied to estimate the top electrode voltage used for computer simulation.

4. Conclusions

Based on the equations developed in the previous study, the anode and measured currents were used to quickly estimate the top electrode voltages for computer simulation when soybeans of different moisture contents were treated in RF systems. The results showed that the top electrode voltage increased almost linearly with increasing moisture content or decreasing electrode gap. The maximum difference of the estimated top electrode voltages between the anode current and the measured current in the same conditions was less than 10% relative error. The top electrode voltages estimated by the developed equations were accurate in computer simulation for RF heated soybeans at different moisture levels. Further validation studies could be conducted to make sure that the developed equations can be applied for other agricultural products.

Acknowledgements

This research was conducted in College of Mechanical and Electronic Engineering, Northwest A&F University, Yangling, China. This research was supported by research grants from PhD Programs Foundation of Ministry of Education in China (20120204110022) and General Program of National Natural Science Foundation in China (No. 31371853). We gratefully thank Zhi Huang, Rongjun Yan, Bo Ling, Lixia Hou and Rui Li for their helps on data processing and suggestions to improve experimental design.

REFERENCES

Alam, A., & Shove, G. (1973). Hygroscopicity and thermal properties of soybeans. *Transactions of the ASAE, 16*(4), 707–709.

Alfaifi, B., Tang, J., Jiao, Y., Wang, S., Rasco, B., Jiao, S., et al. (2014). Radio frequency disinfestation treatments for dried fruit: model development and validation. *Journal of Food Engineering, 120*, 268–276.

Barber, H. (1983). *Electroheat* (1st ed.). London: Granada Publishing Limited.

Birla, S. L., Wang, S., & Tang, J. (2008). Computer simulation of radio frequency heating of model fruit immersed in water. *Journal of Food Engineering, 84*(2), 270–280.

Birla, S., Wang, S., Tang, J., & Hallman, G. (2004). Improving heating uniformity of fresh fruit in radio frequency treatments for pest control. *Postharvest Biology and Technology, 33*(2), 205–217.

COMSOL material library, COMSOL Multiphysics, V4.2a.(2012). Burlington, MA, USA.

Deshapande, S. D., & Bal, S. (1999). Specific heat of soybean. *Journal of Food Process Engineering, 22*(6), 469–477.

Deshapande, S. D., Bal, S., & Ojha, T. P. (1996). Bulk thermal conductivity and diffusivity of soybean. *Journal of Food Process Engineering, 20*(3), 177–189.

Farag, K. W., Lyng, J. G., Morgan, D. J., & Cronin, D. A. (2008). Dielectric and thermophysical properties of different beef meat blends over a temperature range of −18 to +10 °C. *Meat Science, 79*(4), 740–747.

Farag, K. W., Lyng, J. G., Morgan, D. J., & Cronin, D. A. (2011). A comparison of conventional and radio frequency thawing of beef meats: effects on product temperature distribution. *Food and Bioprocess Technology, 4*(7), 1128–1136.

Fu, Y. C. (2004). Fundamentals and industrial applications of microwave and radio frequency in food processing. In J. S. Smith, & Y. H. Hui (Eds.), *Food processing: Principles and applications* (pp. 79–100). Iowa: Blackwell.

Gao, M., Tang, J., Villa-Rojas, R., Wang, Y., & Wang, S. (2011). Pasteurization process development for controlling Salmonella in in-shell almonds using radio frequency energy. *Journal of Food Engineering, 104*(2), 299–306.

Guo, W., Tiwari, G., Tang, J., & Wang, S. (2008). Frequency, moisture and temperature-dependent dielectric properties of chickpea flour. *Biosystems Engineering, 101*(2), 217–224.

Guo, W., Wang, S., Tiwari, G., Johnson, J. A., & Tang, J. (2010). Temperature and moisture dependent dielectric properties of legume flour associated with dielectric heating. *LWT – Food Science and Technology, 43*(2), 193–201.

Huang, Z., Yan, R., Li, R., Zhu, H., Ling, B., & Wang, S. (2014). Finite element analysis on fruit temperature fields based on postharvest disinfestations with hot air and water treatments. *Transactions of the CSAE, 30*(2), 252–259.

Huang, Z., Zhu, H., Yan, R., & Wang, S. (2015). Simulation and prediction of radio frequency heating in dried soybeans for thermal disinfestations. *Biosystems Engineering, 129C*, 34–47.

Jiao, S., Johnson, J. A., Tang, J., & Wang, S. (2012). Industrial-scale radio frequency treatments for insect control in lentils. *Journal of Stored Products Research, 48*, 143–148.

Jiao, Y., Tang, J., Wang, S., & Koral, T. (2014). Influence of dielectric properties on the heating rate in free-running oscillator radio frequency systems. *Journal of Food Engineering, 120*, 197–203.

Kim, S. Y., Sagong, H. G., Choi, S. H., Ryu, S., & Kang, D. H. (2012). Radio-frequency heating to inactivate Salmonella Typhimurium and *Escherichia coli* O157:H7 on black and red pepper spice. *International Journal of Food Microbiology, 153*(1–2), 171–175.

Koral, T. (2004). Radio frequency heating and post-baking. *Biscuit World, 7*(4).

Koray, P. T., Coşkun, Y., Kocadağlı, T., & Gökmen, V. (2012). Effect of radio frequency postdrying of partially baked cookies on acrylamide content, texture, and color of the final product. *Journal of Food Science, 77*(5), E113–E117.

Lagunas-Solar, M., Pan, Z., Zeng, N., Truong, T., Khir, R., & Amaratunga, K. (2007). Application of radiofrequency power for non-chemical disinfestation of rough rice with full retention of quality attributes. *Applied Engineering in Agriculture, 23*(5), 647.

Lee, N.-H., Li, C., Zhao, X.-F., & Park, M.-J. (2010). Effect of pretreatment with high temperature and low humidity on drying time and prevention of checking during radio-frequency/vacuum drying of Japanese cedar pillar. *Journal of Wood Science, 56*(1), 19–24.

Liu, Y., Yang, B., & Mao, Z. (2010). Radio frequency technology and its application in agro-product and food processing. *Transactions of the CSAE, 41*(8), 115–120.

Marshall, M. G., & Metaxas, A. C. (1998). Modeling of the radio frequency electric field strength developed during the RF assisted heat pump drying of particulates. *Journal of Microwave Power and Electromagnetic Energy, 33*(3), 167–177.

Marshall, M. G., & Metaxas, A. C. (1999). Radio frequency assisted heat pump drying of crushed brick. *Applied Thermal Engineering, 19*(4), 375–388.

Metaxas, A. (1996). *Foundations of electroheat: A unified approach* (1st ed.). UK: Wiley Chichester.

Piyasena, P., Dussault, C., Koutchma, T., Ramaswamy, H. S., & Awuah, G. B. (2003). Radio frequency heating of foods: principles, applications and related properties—a review. *Critical Reviews in Food Science and Nutrition, 43*(6), 587–606.

Rani, P. R., Chelladurai, V., Jayas, D. S., White, N. D. G., & Kavitha-Abirami, C. V. (2013). Storage studies on pinto beans under different moisture contents and temperature regimes. *Journal of Stored Products Research, 52*, 78–85.

Shrestha, B., & Baik, O.-D. (2013). Radio frequency selective heating of stored-grain insects at 27.12 MHz: a feasibility study. *Biosystems Engineering, 114*(3), 195–204.

Tiwari, G., Wang, S., Birla, S., & Tang, J. (2008). Effect of water-assisted radio frequency heat treatment on the quality of 'Fuyu'persimmons. *Biosystems Engineering, 100*(2), 227–234.

Tiwari, G., Wang, S., Tang, J., & Birla, S. L. (2011). Computer simulation model development and validation for radio frequency (RF) heating of dry food materials. *Journal of Food Engineering, 105*(1), 48–55.

Uyar, R., Erdogdu, F., & Marra, F. (2014). Effect of load volume on power absorption and temperature evolution during radio-frequency heating of meat cubes: a computational study. *Food and Bioproducts Processing, 92*(3), 243–251.

Wang, S., Birla, S. L., Tang, J., & Hansen, J. D. (2006). Postharvest treatment to control codling moth in fresh apples using water assisted radio frequency heating. *Postharvest Biology and Technology, 40*(1), 89–96.

Wang, S., Luechapattanaporn, K., & Tang, J. (2008). Experimental methods for evaluating heating uniformity in radio frequency systems. *Biosystems Engineering, 100*(1), 58–65.

Wang, S., Monzon, M., Johnson, J. A., Mitcham, E. J., & Tang, J. (2007a). Industrial-scale radio frequency treatments for insect control in walnuts. *Postharvest Biology and Technology, 45*(2), 240–246.

Wang, S., Monzon, M., Johnson, J. A., Mitcham, E. J., & Tang, J. (2007b). Industrial-scale radio frequency treatments for insect control in walnuts. *Postharvest Biology and Technology, 45*(2), 247–253.

Wang, S., Tang, J., & Cavalieri, R. (2001). Modeling fruit internal heating rates for hot air and hot water treatments. *Postharvest Biology and Technology, 22*(3), 257–270.

Wang, S., Tang, J., Johnson, J. A., & Cavalieri, R. P. (2013). Heating uniformity and differential heating of insects in almonds associated with radio frequency energy. *Journal of Stored Products Research, 55*, 15–20.

Wang, S., Tiwari, G., Jiao, S., Johnson, J. A., & Tang, J. (2010). Developing postharvest disinfestation treatments for legumes using radio frequency energy. *Biosystems Engineering, 105*(3), 341–349.

Wang, S., Yue, J., Tang, J., & Chen, B. (2005). Mathematical modelling of heating uniformity for in-shell walnuts subjected to radio frequency treatments with intermittent stirrings. *Postharvest Biology and Technology, 35*(1), 97–107.

Wang, Y., Zhang, L., Johnson, J., Gao, M., Tang, J., Powers, J. R., et al. (2013). Developing hot air-assisted radio frequency drying for in-shell macadamia nuts. *Food and Bioprocess Technology, 7*(1), 278–288.

Zhu, H., Huang, Z., & Wang, S. (2014). Experimental and simulated top electrode voltage in free-running oscillator radio frequency systems. *Journal of Electromagnetic Waves and Applications, 28*(5), 606–617.